Formation of Ethylene-Bridged Dinuclear Ir^{III} Species via M−C Coupling of Ir^{II} and Ir^{II}(ethene)

Bas de Bruin,* Simone Thewissen, Tsi-Wai Yuen, Theo P. J. Peters, Jan M. M. Smits, and Anton W. Gal

Department of Inorganic Chemistry, University of Nijmegen, Toernooiveld 1, 6525 ED Nijmegen, The Netherlands

Received June 19, 2002

Summary: Ethene dissociation from [(Me$_n$tpa)Ir^{II}(ethene)]$^{2+}$, induced by coordination of acetonitrile, causes a rapid and selective M−C coupling between Ir^{II} and Ir^{II}(ethene), resulting in ethylene-bridged dinuclear iridium(III) complexes of the composition [{(Me$_n$tpa)Ir^{III}(NCMe)}$_2$(μ_2-C_2H_4)]$^{4+}$ (n = 2, 3).

Mononuclear complexes of rhodium(II) and in particular iridium(II) are rare.[1,2] Most of the reported Rh^{II} complexes are stabilized by bulky dianionic porphyrinate ligands (por^{2-}). [(Por)Rh^{II}] complexes show a remarkable reactivity toward a variety of otherwise rather inert substrates. Activation under mild conditions of H_2, Si−H and Sn−H bonds, benzylic and allylic C−H bonds, and even methane have been reported.[1a]

[(por)M^{II}(ethene)] species (M = Rh,[1] Ir,[2a] por^{2-} = bulky *meso*-tetraarylporphyrinate dianion), formed in situ from [(por)M^{II}] and ethene, have been reported to undergo bimolecular M−C coupling reactions to form (diamagnetic) ethylene-bridged species [(por)M−CH_2−CH_2−M(por)] and, upon increase of the steric bulk of the por^{2-} ligand, C−C coupling reactions to form butylene-bridged species [(por)M−$CH_2CH_2CH_2CH_2$−M(por)]. Apparently, in [(por)M^{II}(ethene)] the unpaired electron has a relatively high density on the ethene substrate, imposing some M^{III}−ethyl radical character on these transient species.[1]

Recently we reported the formation of [(Me$_3$tpa)Ir^{II}(ethene)]$^{2+}$ (**2**), the first example of a *stable* Ir^{II}−ethene complex.[3] Complex **2** (Scheme 1) was synthesized by oxidation of [(Me$_3$tpa)Ir^{I}(ethene)]$^{+}$ (**1**)[4] with ferrocenium hexafluorophosphate ([Fc]PF_6). DFT calculations indicated that the unpaired electron density of **2** is partially located on the ethene fragment. Quite remarkably, however, complex **2** did *not* spontaneously dimerize via C−C radical coupling to a butylene-bridged dinuclear complex.

Scheme 1. Preparation of [(Me$_n$tpa)Ir^{II}(ethene)]$^{2+}$ (*n* = 2, 3)

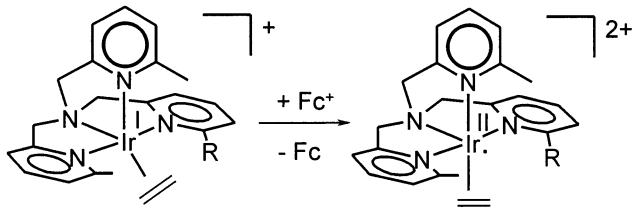

1: R= Me
3: R= H

2: R= Me
4: R= H

Complex **2** does not react with carbon monoxide on bubbling CO through a solution of [**2**]$(PF_6)_2$ in acetone at room temperature. This is surprising in view of the reported higher affinity of [(por)Rh^{II}] for CO relative to ethene.[5] The metal center of **2** is shielded by the three methyl groups at the pyridine 6-positions of the Me$_3$-tpa ligand,[6] and substitution of ethene might well be kinetically hampered. In an attempt to increase the accessibility of the vacant sixth coordination site at iridium, we studied [(Me$_2$tpa)Ir^{II}(ethene)]$^{2+}$ (**4**), the less hindered analogue of **2**.

The iridium(II)−ethene complex **4**[7] (Scheme 1; R = H) was synthesized by a procedure similar to that reported for **2**:[3] i.e., one-electron oxidation of the iridium(I)−ethene precursor [(Me$_2$tpa)Ir^{I}(ethene)]$^{+}$ (**3**) [8] with [Fc]PF_6 in dichloromethane. The EPR spectrum[7] of **4** in acetone/MeOH (2:3) is virtually identical with that of **2**.[3]

For the redox couple **1**/**2** electrochemically reversible oxidation−reduction waves (ΔE = 68−70 mV, I_b/I_f = 1.0) were observed with cyclic voltammetry in CH_2Cl_2, acetone, and MeCN. The redox couple **3**/**4** also gives rise

* To whom correspondence should be addressed. Fax: +31 24 355 34 50. Tel: +31 24 365 2464. E-mail: BdeBruin@sci.kun.nl.

(1) For an overview see: (a) DeWit, D. G. *Coord. Chem. Rev.* **1996**, *147*, 209−246. (b) Pandey, K. K. *Coord. Chem. Rev.* **1992**, *121*, 1−42. (c) Bunn, A.; Wayland, B. B. *J. Am. Chem. Soc.* **1992**, *114*, 6917−6919 and references therein.

(2) For recent examples of mononuclear iridium(II) complexes, see: (a) Zhai, H. L.; Bunn, A.; Wayland, B. B. *Chem. Commun.* **2001**, 1294−1295. (b) Collman, J. P.; Chang, L. L.; Tyvoll, D. A. *Inorg. Chem.* **1995**, *34*, 1311−1324. (c) Garcia, M. P.; Jimenez, M. V.; Oro, L. A.; Lahoz, F. J.; Alonso, P. J. *Angew. Chem., Int. Ed. Engl.* **1992**, *31*, 1527−1529. (d) Garcia, M. P.; Jimenez, M. V.; Oro, L. A.; Lahoz, F. J.; Tiripicchio, M. C.; Tiripicchio, A. *Organometallics* **1993**, *12*, 4660−4663. (e) Bond, A. M.; Humphrey, D. G.; Menglet, D.; Lazarev, G. G.; Dickson, R. S.; Vu, T. *Inorg. Chim. Acta* **2000**, *300*, 565−571. (f) Danopoulos, A. A.; Wilkinson, G.; Hussainbates, B.; Hursthouse, M. B. *J. Chem. Soc., Dalton Trans.* **1992**, 3165−3170.

(3) de Bruin, B.; Peters, T. P. J.; Thewissen, S.; Blok, A. N. J.; Wilting, J. B. M.; de Gelder, R.; Smits, J. M. M.; Gal, A. W. *Angew. Chem., Int. Ed.* **2002**, *41*(12), 2135−2138.

(4) de Bruin, B.; Peters, T. P. J.; Wilting, J. B. M.; Thewissen, S.; Smits, J. M. M.; Gal, A. W. *Eur. J. Inorg. Chem.*, in press.

(5) Basickes, L.; Bunn, A. G.; Wayland, B. B. *Can. J. Chem.* **2001**, *79*, 854−856.

(6) Nagao, H.; Komeda, N.; Mukaida, M.; Suzuki, M.; Tanaka, K. *Inorg. Chem.* **1996**, *35*, 6809−6815.

(7) Data for **4**: EPR (9.299 GHz, acetone/MeOH (2:3), 40 K) g_{11} = 2.52 (five-line pattern (1:4:6:4:1), $A_{11} \approx$ 175 MHz), g_{22} = 2.27 (no resolved hyperfine couplings), g_{33} = 1.98 (A_{33}^{Ir} = 129 MHz, A_{33}^{N} = 55 MHz). Anal. Calcd for $C_{22}H_{26}N_4IrP_2F_{12}$: C, 31.89; H, 3.16; N, 6.76. Found: C, 31.59; H, 3.20; N, 6.59.

(8) The synthesis of **3** follows procedures similar to those reported for **1**,[4] using Me$_2$tpa instead of Me$_3$tpa.[6] Data for **3**: ^{1}H NMR (acetone-d_6, 298 K) δ 8.40 (1H, d, Py-H6), 7.75−7.05 (9H, Py *H3*, Py *H4*, and Py *H5*), 5.62−4.65 (6H, 6 × d[AB], N−CH_2−Py), 3.53 (s, 3H, Py−CH_3), 2.85 (s, 3H, Py−CH_3), 1.85 (m, 1H, CH_2=CH_2), 1.5−1.2 (m, 3H, CH_2=CH_2); ^{13}C NMR (CD_2Cl_2, 298 K) δ {165.4, 164.9, 164.0, 160.7, 160.3, 151.0, 137.2, 136.9, 135.5, 125.1, 125.0, 124.0, 122.2, 120.6, 119.4} (Py C2, C3, C4, C5, and C6), {72.4, 70.4, 65.9} (N−CH_2−Py), {30.4, 27.8} (Py−CH_3), {4.04, 2.87} (CH_2=CH_2). Anal. Calcd for $C_{22}H_{26}N_4IrPF_6$: C, 38.65; H, 3.83; N, 8.20. Found: C, 38.56; H, 3.86; N, 8.08.

10.1021/om020476m CCC: $22.00
Publication on Web 09/20/2002

Table 1. Electrochemical Data for [(Me_ntpa)Ir^I(ethene)]$^+$ (n = 0−3)[a]

compd	solvent	E_p[a]	$E_{1/2}$	ΔE	I_b/I_f
[(Me_3tpa)Ir^I(ethene)]$^+$ (**1**)	CH_2Cl_2	−255	−289	68	1.0
[(Me_3tpa)Ir^I(ethene)]$^+$ (**1**)	acetone	−334	−368	70	1.0
[(Me_3tpa)Ir^I(ethene)]$^+$ (**1**)	MeCN	−330	−365	69	1.0
[(Me_2tpa)Ir^I(ethene)]$^+$ (**3**)	CH_2Cl_2	−138	−173	68	1.0
[(Me_2tpa)Ir^I(ethene)]$^+$ (**3**)	acetone	−213	−249	70	1.0
[(Me_2tpa)Ir^I(ethene)]$^+$ (**3**)	MeCN	−198	−240	84	0.4
[(Me_1tpa)Ir^I(ethene)]$^+$	CH_2Cl_2	−43			0
[(Me_1tpa)Ir^I(ethene)]$^+$	acetone	−122			0
[(Me_1tpa)Ir^I(ethene)]$^+$	MeCN	−93			0
[(tpa)Ir^I(ethene)]$^+$	CH_2Cl_2	−136			0
[(tpa)Ir^I(ethene)]$^+$	acetone	−144			0
[(tpa)Ir^I(ethene)]$^+$	MeCN	−10			0

[a] E is given in mV versus Fc/Fc^+. E_p[a] = anodic peak potential, $E_{1/2}$ = half-wave potential, ΔE = peak separation, I_b/I_f = cathodic peak current/anodic peak current.

to reversible waves in CH_2Cl_2 and acetone, but oxidation of **3** in MeCN is almost completely irreversible (I_b/I_f = 0.4). Apparently, **4** has a reduced stability in MeCN compared to the less coordinating solvents acetone and CH_2Cl_2 (Table 1).

Less substituted analogues of **3**, viz. [(Metpa)Ir^I(ethene)]$^+$ and [(tpa)Ir^I(ethene)]$^+$,[9,10] reveal entirely irreversible oxidation waves even in the weakly coordinating solvents CH_2Cl_2 and acetone (Table 1). In line with these observations, any attempts to prepare the corresponding iridium(II)−ethene species (less substituted analogues of **2** and **4**) were not successful. Apparently, steric shielding of the iridium(II) center is important to stabilize iridium species in the unusual oxidation state +2, and thus [(Me_ntpa)Ir^{II}(ethene)]$^{2+}$ could be isolated for n = 3 and n = 2 but not for n = 1 or n = 0.

In good agreement with the electrochemical data, both **2** and **4** are quite stable in acetone, judging from the persistence of their paramagnetically shifted ^{1}H NMR signals. Complex **2** is entirely stable in acetone (>48 h), but a slight degradation of **4** was observed after 2 h at room temperature. Complete degradation of **4** in acetone requires more than 24 h and results in a complex mixture of diamagnetic products. This process is accelerated upon passing either N_2 or CO gas through the solution (complete degradation within 30 min) and is therefore probably related to ethene loss.

In MeCN complex **2** is moderately stable and slowly and selectively converts to diamagnetic product **5**.[11] Full conversion of **2** to **5** requires approximately 90 min. Complex **4** is more reactive in MeCN and instantaneously and selectively converts to a 1:1 mixture of the diamagnetic products **6a** and **6b** (Scheme 2).[12]

The constitution of **5** and **6a**/**6b**, being ethylene-bridged dinuclear complexes of composition [(Me_ntpa)-

Scheme 2. Formation of Ethylene-Bridged Dinuclear Species from [(Me_ntpa)Ir^{II}(ethene)]$^{2+}$ (n = 2, 3) in MeCN

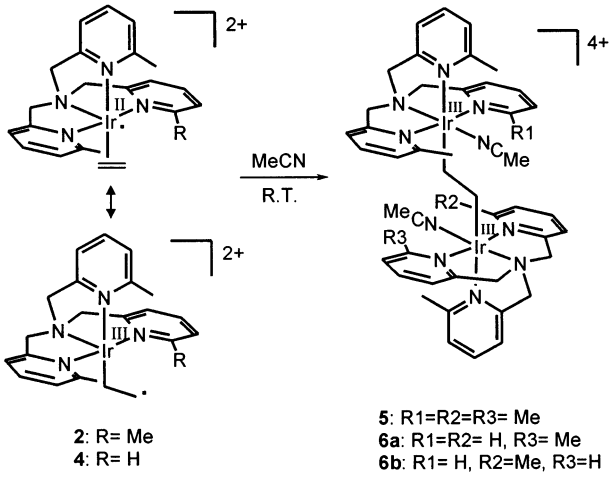

(MeCN)M^{III}−CH_2CH_2−M^{III}(NCMe)(Me_ntpa)]$^{4+}$ (**5**, n = 3; **6a**/**6b**, n = 2) was derived from NMR and ESI-MS data. Due to the chirality of **4**, the dinuclear complex **6** is formed as 1:1 mixture of the two diastereomers **6a** (*rac*, C_2 symmetric) and **6b** (*meso*, C_i symmetric), of which **6b**[13] preferentially crystallized from MeCN/MeOH (Scheme 2).

Thus, whereas **2** and **4** are relatively stable in weakly coordinating solvents such as acetone and CH_2Cl_2, the stronger donor MeCN apparently triggers ethene dissociation and M−C coupling of Ir^{II} and Ir^{II}(ethene). The observation that the reaction rate increases on going from the Me_3tpa complex **2** to the more accessible Me_2-tpa complex **4** suggests that the reaction proceeds via an associative mechanism.

In view of the radical type mechanisms proposed for formation of the species [(por)M−CH_2CH_2−M(por)] and [(por)M−$CH_2CH_2CH_2CH_2$−M(por)] from [(por)M^{II}] and ethene,[1c] it is tempting to propose a similar radical pathway for formation of **5** and **6a**/**6b** (Scheme 3). Rate-limiting substitution of ethene by MeCN via an associative (A) or associative interchange (I_a) mechanism could be followed by a radical coupling of Ir^{II} and Ir^{II}(ethene). The associative substitution at these Me_ntpa−iridium-(II) centers would thus require "hard" donors (e.g. MeCN), since **2** and **4** do not seem to have an affinity for CO (vide infra).

Clearly the Ir^{III}−ethyl radical character of **2** and **4** is insufficient to support a C−C radical coupling to butylene-bridged dinuclear species, but M−C radical coupling with in situ generated (more reactive) metal-centered radicals [(Me_ntpa)Ir^{II}(NCMe)]$^{2+}$ could well be

(9) Krom, M.; Peters, T. P. J.; Coumans, R. G. E.; Sciarone, T. J. J.; Hoogboom, J. T. V.; ter Beek, S. I.; Schlebos, P. P. J.; Smits, J. M. M.; de Gelder, R.; Gal, A. W. Submitted for publication in *Eur. J. Inorg. Chem.*

(10) Kicken, R. J. N. A. M. Oxidation of Iridium Olefin Complexes by H_2O_2 and O_2, Thesis, University of Nijmegen, 2001.

(11) Data for **5**: ^{1}H NMR (CD_3CN, 298 K) δ 7.9−7.1 (18H, Py *H3*, Py *H4*, and Py *H5*), 4.78 (4H, d[AB], 16.4 Hz, N−CH_2−Py), 4.55 (4H, d[AB], 16.4 Hz, N−CH_2−Py), 4.54 (4H, s, N−CH_2−Py), 3.02 (6H, s, Py−CH_3), 2.72 (s, 6H, IrNC−CH_3), 2.68 (12H, s, Py−CH_3), 2.17 (4H, s, Ir−CH_2CH_2−Ir); ^{13}C NMR (CD_3CN, 298 K) δ {165.5, 163.8, 162.5, 157.5, 140.6, 140.1, 128.3, 127.5, 124.3, 122.0, 120.4} (Py C2, C3, C4, C5, and C6), {74.4, 70.7} (N−CH_2−Py), {27.1, 26.7} (Py−CH_3), 5.03 (NCCH_3), 3.05 (Ir−CH_2CH_2−Ir), NCCH_3 signal obscured by the solvent signal. Anal. Calcd for $C_{48}H_{59}N_{11}Ir_2P_4F_{24}$: C, 32.62; H, 3.78; N, 8.62. Found: C, 33.54; H, 3.47; N, 8.68.

(12) NMR signals of **6a** partially overlap with those of **6b**, but separated signals for Py *H6*, Py−*Me*, Ir−NCCH_3, and Ir−CH_2CH_2−Ir fragments clearly reveal the presence of **6a** in equimolar amounts with **6b**.

(13) Data for **6b**: ^{1}H NMR (CD_3CN, 298 K) δ 8.45 (2H, d, Py H6), 7.94−7.16 (18H, Py *H3*, Py *H4*, and Py *H5*), 4.85−4.30 (12H, six [AB]-type doublets, N−CH_2−Py), 2.92 (s, 6H, Py−CH_3), 2.78 (s, 6H, Py−CH_3), 2.71 (s, 6H, IrNC−CH_3), 1.68 (2H, m, AA′BB′, Ir−CH_2CH_2−Ir), 1.55 (2H, m, AA′BB′, Ir−CH_2CH_2−Ir); ^{13}C NMR (CD_3CN, 298 K) δ {165.3, 164.2, 162.9, 162.3, 157.5, 150.9, 140.8, 140.7, 140.4, 127.6, 127.2, 124.5, 122.7, 120.5} (Py C2, C3, C4, C5, and C6), {75.0, 70.6, 70.4} (N−CH_2−Py), {27.9, 26.7} (Py−CH_3), 5.26 (NCCH_3), 4.98 (Ir−CH_2CH_2−Ir), NCCH_3 signal obscured by the solvent signal. Anal. Calcd for $C_{46}H_{54}N_{10}Ir_2P_4F_{24}$: C, 32.29; H, 3.18; N, 8.18. Found: C, 32.11; H, 3.24; N, 8.12.

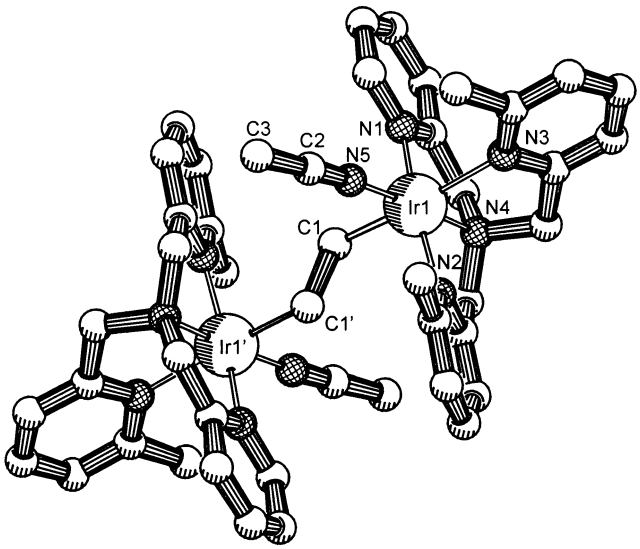

Figure 1. X-ray structure of **6b** (all hydrogen atoms omitted). Selected bond lengths (Å) and angles (deg): Ir1−N1 = 2.041(5), Ir1−N2 = 2.073(5), Ir1−N3 = 2.257(5), Ir1−N4 = 2.034(5), Ir1−N5 = 2.020(5), Ir1−C1 = 2.116(5), C1−C1′ = 1.510(11), N5−C2 = 1.135(7), C2−C3 = 1.446(8); Ir1−C1−C1′ = 118.0(5). Corresponding bond lengths (Å) and angles (deg) for **5**: Ir1−N1 = 2.093(4), Ir1−N2 = 2.103-(5), Ir1−N3 = 2.270(4), Ir1−N4 = 2.041(4), Ir1−N5 = 2.007(4), Ir1−C1 = 2.105(5), C1−C1′ = 1.501(7), N5−C2 = 1.138(7), C2−C3 = 1.445(8); Ir1−C1−C1′ = 117.7(4).

Scheme 3. Proposed Mechanism for Formation of 5 and 6a/6b

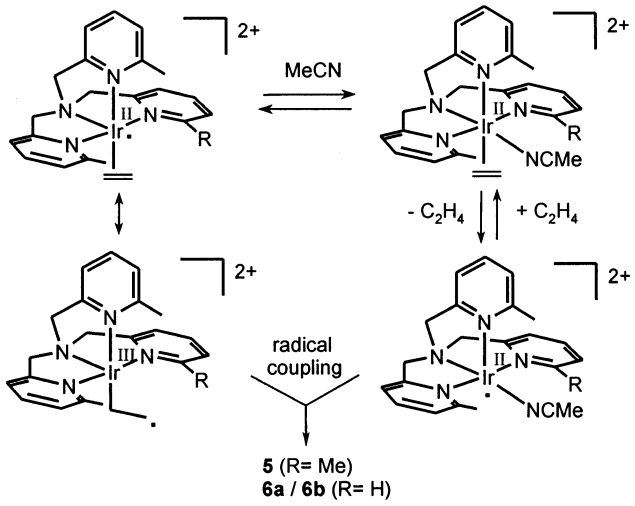

a route to the ethylene-bridged species **5** and **6a**/**6b** (Scheme 3). However, in the absence of further evidence, we cannot exclude alternative mechanisms. For example, electron transfer (induced by coordination of MeCN) might generate intermediate Ir^{I} and Ir^{III} species which couple via electrophilic attack of Ir^{III} at Ir^{I}(ethene) or nucleophilic attack of Ir^{I} at Ir^{III}(ethene), thus forming **5** and **6a**/**6b**.

The irreversible oxidation of $[(Metpa)Ir^{I}(ethene)]^{+}$ and $[(tpa)Ir^{I}(ethene)]^{+}$ in MeCN, as observed with cyclic voltammetry, is probably related to a rapid M−C coupling reaction similar to the conversion of **2** and **4** in MeCN to **5** and **6**, respectively. Preliminary ^{1}H NMR experiments indicated formation of $[\{(Me_ntpa)Ir^{III}(NCMe)\}_2(\mu_2\text{-}C_2H_4)]^{4+}$ (n = 0, 1) upon in situ oxidation of $[(Me_ntpa)Ir^{I}(ethene)]^{+}$ (n = 0, 1) with Fc^{+} in MeCN.

Crystals of **5** (not shown) and **6b** suitable for X-ray diffraction were obtained from DMSO/MeOH.[14] The X-ray structure of **6b** is shown in Figure 1.

Although [(por)M−CH_2CH_2−M(por)] (M = Rh, Ir) species have been reported for a variety of por^{2-} ligands, none of these have been structurally characterized by X-ray diffraction. The structures of **5** and **6b** clearly reveal the μ_2-η^1:η^1 linkage of the $C_2H_4^{2-}$ fragment, thus providing support for the proposed structures of [(por)M−CH_2CH_2−M(por)] (M = Rh, Ir).

It is useful to compare the chemistry of $[(por)M^{II}]$ (M = Rh, Ir) and Me_ntpa−iridium(II) complexes here. In both systems, steric shielding is the key to control over stability and reactivity. The ethene complexes appear to have at least some ligand radical character. However, the Me_ntpa complexes have more affinity for σ-donor ligands (nitrile), whereas the por^{2-} complexes seem to prefer π-acceptor ligands (CO).[5] This difference might be due to the stronger donor character of the anionic por^{2-} ligands compared to the neutral Me_ntpa ligands. Finally, the coordination geometries of the two systems are completely different. In contrast to Me_ntpa, the por^{2-} ligands maintain trans vacant sites and thus do not allow cis reactivity patterns of substrate fragments. We therefore expect to find marked differences in reactivity between the radical species $[(Me_ntpa)M^{II}]$ and $[(por)M^{II}]$ in future studies.

Supporting Information Available: Figures giving ORTEP representations and tables of crystallographic data for **5** and **6b**, as well as crystallographic data in CIF format. This material is available free of charge via the Internet at http://pubs.acs.org.

OM020476M

(14) Diffraction experiments were performed on an Enraf-Nonius CAD4 using graphite-monochromated Mo Kα radiation (λ = 0.710 73 Å). The structures were solved using the PATTY option (Beurskens, P. T.; Beurskens, G.; Strumpel, M.; Nordman, C. E. In *Patterson and Pattersons*; Clarendon: Oxford, U.K., 1987; p 356) of the DIRDIF-96 program system (Beurskens, P. T.; Beurskens, G.; Bosman, W. P.; de Gelder, R.; García-Granda, S.; Gould, R. O.; Israël, R.; Smits, J. M. M. University of Nijmegen, The Netherlands, 1996). Refinements (full-matrix least squares on F^2) were carried out with the SHELXL-97 package (Sheldrick, G. M. SHELXL-97; University of Göttingen, Göttingen, Germany, 1997). Geometry calculations were performed with the PLATON-93 program (Spek, A. L. PLATON-93; University of Utrecht, Utrecht, The Netherlands, 1995) and revealed neither unusual geometric features nor unusually short intermolecular contacts. The calculations revealed no higher symmetry and no (further) solvent-accessible areas. Crystal data for **5**: $C_{50}H_{61}F_{24}Ir_2N_{11}P_4$, M_r = 1780.38, triclinic, a = 12.1371(10) Å, b = 14.9716(12) Å, c = 19.096(2) Å, U = 3174.7(5) Å^3, T = 293(2) K, space group $P\bar{1}$, Z = 2, μ(Mo Kα) = 4.404 mm^{-1}, 15 112 reflections measured on an Enraf-Nonius CAD4 diffractometer, of which 14 554 were unique (R_{int} = 0.0204). Final R indices: R1 = 0.0379 (for 11 003 reflections considered observed ($I > 2\sigma(I)$), wR2 = 0.0966 (all data). A few atoms of one pyridyl fragment of one ligand, C53, C54, and C55, showed large disorder and were split into two partially occupied parts. Even then, one of the two parts still shows large disorder, but further splitting does not improve the physical model. The same holds for some of the anion fluorine atoms, for which no other models could be found that would result in a stable refinement. Crystal data for **6b**: $C_{25}H_{33}N_5OSIrP_2F_{12}$, M_r = 933.76, triclinic, a = 12.500(2) Å, b = 12.837(4) Å, c = 13.093(5) Å, U = 1709.0-(9) Å^3, T = 293(2) K, space group $P\bar{1}$, Z = 2, μ(Mo Kα) = 4.155 mm^{-1}, 8189 reflections measured on an Enraf-Nonius CAD4 diffractometer, of which 7831 were unique (R_{int} = 0.0149). Final R indices: R1 = 0.0408 (for 6621 reflections considered observed ($I > 2\sigma(I)$), wR2 = 0.1101 (all data). From the anisotropic thermal displacement parameters for the PF_6 and DMSO moieties it is clear that some atoms show a large positional disorder. Although it is possible to use several partially occupied positions for these atoms, no physically reasonable models result from these parameters, at least none that are any better than the models presented here. The assignment of atomic species in the DMSO moiety is based on bond distances and equivalent isotropic thermal displacement parameters.